so that $\Delta H/H\Delta p \approx \Delta\mu_1/\mu_1\Delta p$. As seen from Fig. 2, this relation agrees with experiments. The contributions made to the polarization of the conduction electrons, and consequently the contributions from the nearest spheres in the AF_1, AF_2, and AF_0 structures are apparently different. The quantity $c\bar{\mu}$ is in fact the sum of the contribution from the coordination spheres with numbers $n \geq 3$, the most substantial of which are the contributions from the third and fourth spheres, and the rest can be neglected. Therefore for most atoms $c\bar{\mu} \neq 0$ in the AF_1 and AF_2 structures, because of the large length of the SDW compared with the lattice period. When this circumstance is taken into account, the values of $\Delta H/H\Delta p$ for AF_1, AF_2, and AF_0 should be different. The accuracies of our measurements, strictly speaking, are insufficient for the observation of these differences, nonetheless the tendency towards such a difference does apparently exist (see Fig. 2).

Our experiments allow us therefore to draw the following conclusions: 1) the hyperfine magnetic fields at impurity iron atoms in chromium are determined by the nearest neighboring chromium atoms, 2) the anomalously large relative changes of the hyperfine fields at the ^{57}Fe nuclei in Cr under pressure are the consequence of changes of the magnetic moments of the chromium atoms.

In conclusion the authors are grateful to V. A. Makarov for kindly supplying the alloy samples and for discussing the result, and V. P. Mar'in for help with the measurements.

[1]L. Gorliss, J. Hastings, and R. J. Weiss, Phys. Lett. **3**, 211 (1959). G. E. Bacon, Acta Crystallogr. **14**, 83 (1961). G. Shirane and W. J. Takei, J. Phys. Soc. Jpn. **17**, 35 (1972). A. Arrot and S. A. Werner, Phys. Rev. **153**, 624 (1967).
[2]V. A. Makarov, B. N. Tret'yakov, I. M. Puzei, G. P. Kalinin, and V. A. Tokmakova, Fiz. Tverd. Tela (Leningrad) **21**, 901 (1979) [Sov. Phys. Solid State **21**, 527 (1979)].
[3]Y. Ishikawa, R. Tournier, and J. Filippi, J. Phys. Chem. Solids **26**, 1727 (1965).
[4]I. R. Herbert, P. E. Clark, and G. V. H. Wilson, J. Phys. Chem. Solids **33**, 979 (1972).
[5]N. A. Blum, Massachussetts Institute of Technology, Technical Report NML 64-2, 1964.
[6]R. B. Frankel and N. A. Blum, J. Phys. Chem. Solids **34**, 1565 (1973).
[7]I. N. Nikolaev, V. P. Potapov, and N. N. Delyagin, Zh. Eksp. Teor. Fiz. **70**, 241 (1976) [Sov. Phys. JETP **43**, 125 (1976)].
[8]C. E. Violet and R. J. Borg, Phys. Rev. **149**, 540 (1966).
[9]H. Umebayashi, G. Shirane, and B. C. Frazer, J. Phys. Soc. Jpn. **24**, 368 (1968).
[10]D. N. Pipkorn, C. K. Edge, P. Debrunner, G. De Pasquali, H. G. Drickamer, and H. Frauenfelder, Phys. Rev. **135**, A1604 (1964). I. N. Nikolaev, V. P. Potapov, I. Yu. Bezotosnyĭ, and V. P. Mar'in, Zh. Eksp. Teor. Fiz. **75**, 346 (1978) [Sov. Phys. JETP **48**, 171 (1978)].
[11]W. N. Lomer, Proc. Phys. Soc. **London 80**, 489 (1962).
[12]M. K. Wilkinson, E. O. Wollan, W. C. Koehler, and J. W. Cable, Phys. Rev. **127**, 2080 (1962).
[13]R. Street and B. Window, Proc. Phys. Soc. London **89**, 587 (1966).
[14]N. N. Delyagin and E. N. Kornienko, Zh. Eksp. Teor. Fiz. **61**, 1946 (1971) [Sov. Phys. JETP **34**, 1036 (1971)].

Translated by J. G. Adashko

Density of states in a one-dimensional disordered crystal

A. A. Gogolin

L. D. Landau Institute of Theoretical Physics, USSR Academy of Sciences
(Submitted 21 May 1979)
Zh. Eksp. Teor. Fiz. 77, 1649–1661 (October 1979)

The Berezinskiĭ diagram technique is used to calculate the density of states in a one-dimensional crystal with a strong degree of disorder. The character of the Dyson singularity at the center of the band is studied. The structure of the state-density peaks produced at rational points of the band is investigated.

PACS numbers: 63.90. + t

1. INTRODUCTION

In connection with the intensive experimental investigations of quasi-one-dimensional crystals with strong structural disorder,[1] theoretical investigations of the electron spectrum in one-dimensional disordered structures have attracted great interest. The state density in such systems was investigated in many studies (see the review[2]). It was found that in one-dimensional problems the state density is very sensitive to the crystal structure. Great interest attaches therefore to allowance for the periodicity of the initial crystal potential. Among the most significant results in this field is the singularity observed by Dyson[3] in the state density near the middle of the band. It was subsequently observed in a large number of systems.[4-6] All the cited studies dealt with the case of weak disorder.

The present paper deals with the density of the electron states in a one-dimensional crystal with arbitrary disorder. It is shown that in this case the state-density peaks appear at all rational points of the band, and that the Dyson singularity at the center of the band is greatly enhanced. These effects are due to the strong Bragg scattering of the electrons in one-dimensional crystals and to the interference of the corresponding waves.

 0038-5646/79/100827-07$02.40

2. DERIVATION OF THE FUNDAMENTAL EQUATIONS

We consider a one-dimensional systems of non-interacting electrons with a dispersion law $\varepsilon(p)$, situated in the field of impurities that are randomly scattered over the sites of a lattice having a period a. We assume that the concentrations of the impurities per site c is small ($c \ll 1$), and that the potential $u(x)$ of a single impurity is arbitrary. To calculate the density $\rho(\varepsilon)$ of the electron states we use the known formula

$$\rho(\varepsilon)=-\pi^{-1}\operatorname{Im}\langle G^{+}(0\,0|\varepsilon)\rangle, \tag{1}$$

where $G^{+}(n_1 n_2|\varepsilon)$ is the retarded Green's function of the electron, n_1 and n_2 are the numbers of the sites, and the angle brackets denote averaging over the locations of the impurities.

We average over the impurity positions by the usual cross technique. In the case of a weak impurity potential it suffices to use the Born approximation for the scattering amplitude and to introduce into the diagrams pairwise connected crosses. The simplest diagram of this type, for the case when the electron energy is close to the middle of the band [$p(\varepsilon)\approx\pi/2a$], is shown in Fig. 1. The wavy lines correspond to the paired correlator of the impurity potential. In the case of a strong potential, further expansion in the Born parameter

$$\alpha=\frac{1}{v(\varepsilon)}\int_{-\infty}^{\infty}u(x)\cos(2p(\varepsilon)x)\,dx$$

[$v(\varepsilon)=d\varepsilon/dp$ is the electron velocity and $p(\varepsilon)$ is its momentum] leads to binding of individual crystals into clusters. Next, in perfect analogy with our preceding paper, we can sum the within the framework of an individual cluster and separate it the total amplitudes f_+ and f_- for forward and backward scattering, respectively. The thin wavy lines on the diagrams are then replaced by thick ones corresponding to the total scattering amplitudes. The thick wave lines are bound into clusters, and this corresponds to multiple scattering of the electron by a single impurity. Depending on the type of vertex (straight or angled) is located at the end of the wave line, the latter corresponds to the backward (f_-) or forward (f_+) scattering amplitude (Fig. 2).

We are interested primarily in the character of the density of the electron states near the middle of the band. We consider therefore first the case $p(\varepsilon)\approx\pi/2a$. This corresponds to retaining in the diagrams the slowly varying factors of the type

$$\exp\{4ip(\varepsilon)x\}=\exp\{4i(p(\varepsilon)-p_0)x\},\qquad p_0=\pi/2a,\quad x=na,$$

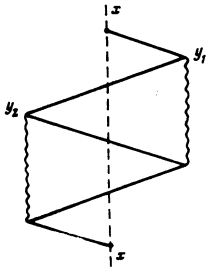

FIG. 1.

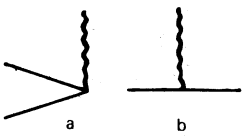

FIG. 2.

and neglecting the diagrams containing rapidly oscillating factors of the type $\exp(ipx)$. This sorting out of the diagrams is carried out in accord with the usual parameter $(p_F l)^{-1}\sim c\ll 1$ (l is the electron mean free path).

Cutting the diagram of Fig. 1 along the xx axis and then shifting the point x, we obtain in analogy with Refs. 6 and 7 the following equation for the right part of the diagram $R_m(x)$:

$$-\frac{d}{dx}R_m=c\sum_s V_{ms}R_{m+s}e^{4i(p_0-p)x}-cR_m+cR_0 f_-^{2m}e^{4i(p-p_0)x}, \tag{2}$$

$$V_{ms}=\sum_k C_{2m}^{k}C_{2m+2s-1}^{k+2s}(f_-)^{2k+2s}(1+f_+)^{4m-2k}; \tag{3}$$

where V_{ms} is the effective expression for a multiple-ended vertex that changes the number of line pairs $2m$ in the section xx by $2s$. The substitution

$$R_m(x)=R_m(-1)^m e^{4i(p-p_0)mx}$$

reduces Eq. (2) to the form

$$-itmR_m=\frac{1}{\gamma}\sum_s V_{ms}R_{m+s}(-1)^s-\frac{1}{\gamma}R_m+R_0\frac{1}{\gamma}(-1)^m f_-^{2m}, \tag{4}$$

where $t=4(p-p_0)l$, $l=1/c\gamma$, $\gamma=|f_-|^2$ is the coefficient of reflection from an individual impurity. Equation (4) must be solved with the boundary condition $R_0=1$.

The density $\rho(\varepsilon)$ of the electronic states is expressed in terms of the R_m in accord with the formula[6]

$$\rho(\varepsilon)=\rho_0(\varepsilon)\left(1+2\operatorname{Re}\sum_{m=1}^{\infty}R_m^2\right), \tag{5}$$

where $\rho_0(\varepsilon)=1/\pi v(\varepsilon)$ is the state density in the absence of impurities.

The complex scattering amplitudes f_+ and f_- are connected by the unitarity relations, which in the one-dimensional case and for a symmetrical potential $u(x)=u(-x)$, with account taken of the additional factors i/v, takes the form[7]

$$-(f_+ + f_+^*)=|f_+|^2+|f_-|^2, \tag{6}$$

$$-(f_- + f_-^*)=f_+f_-^*+f_-f_+^*. \tag{7}$$

From (6) and from the definition of γ it follows that

$$|1+f_+|^2=1-\gamma. \tag{8}$$

We obtain similarly from (7)

$$f_-(1+f_+^*)=-f_-^*(1+f_+). \tag{9}$$

Using relations (8) and (9) and defining the phase φ and the amplitude $1+f_+$ by the relation $1+f_+=(1-\gamma)^{1/2}e^{i\varphi}$, we reduce Eq. (4) to the form

$$-itmR_m=\frac{1}{\gamma}\sum_s V_{ms}R_{m+s}(-1)^s-\frac{1}{\gamma}R_m+\gamma^{m-1}e^{2im\varphi}, \tag{10}$$

$$V_{ms}=\sum_k C_{2m}^{k}C_{2m+2s-1}^{k+2s}(-\gamma)^{k+s}(1-\gamma)^{2m-k}e^{2i\varphi(2m+s)}. \tag{11}$$

By solving (10) we obtain the function $\rho(t)$ for different values of γ and φ.

3. SCATTERING AMPLITUDE

Of greatest physical interest is the case $\varphi = 0$. As will be shown below, at $\varphi = 0$ the Dyson instability of the state density $\rho(\varepsilon) \propto |\varepsilon \ln^3 \varepsilon|^{-1}$ appears at the center of the band. A situation with zero forward-scattering phase occurs in a system with purely nondiagonal disorder, as well as for a number of potentials considered in the present paper. Gor'kov and Dorokhov[8] have shown that this property is possessed by the random potential produced by the structural disorder in TCNQ salts with asymmetric cations. The case of a purely nondiagonal disorder is of considerable interest, since one can reduce to it many problems connected with the calculation of the density of spin and phonon states in disordered chains.[9] We shall show that scattering of quasiparticles in such systems corresponds to $\varphi = 0$.

We consider to this end the usual Hamiltonian of the motion of a quasiparticle over a one-dimensional lattice in the tight-binding approximation:

$$H = \sum_{m,n} M_{nm} \psi_m^+ \psi_n, \quad M_{nm} = M_{mn}. \tag{12}$$

The Schrödinger equation for the wave function u_n takes in the discrete representation the form

$$\sum_m M_{nm} u_m = \varepsilon u_n, \tag{13}$$

where ε is the quasiparticle energy.

We consider the case when the hopping matrix elements differ from zero only for the nearest neighbors, and assume that they are constant along the entire chain with the exception of the transition between the zeroth and first sites. In this case

$$M_{nm} = M(\delta_{n,m+1} + \delta_{n+1,m}) + \beta(\delta_{n0}\delta_{m1} + \delta_{n1}\delta_{m0}), \tag{14}$$

where $M + \beta$ is the overlap integral between the zeroth and first sites, and M is the overlap integral between the remaining sites. Substituting in (13) u_n in the form

$$u_n = e^{ikan} + Ae^{ika|n|} + Be^{ika|n-1|}, \tag{15}$$

we get

$$A = -\beta \frac{2iM \sin ka + \beta(e^{2ika} - 1)}{(2iM \sin ka + \beta e^{ika})^2 - \beta^2}, \tag{16}$$

$$B = -\beta \frac{2iM \sin ka + \beta(e^{ika} - i)}{(2iM \sin ka + \beta e^{ika})^2 - \beta^2}. \tag{17}$$

Near the center of the band we can put in (16) and (17) $ka = \pi/2$, as a result of which the expression for the amplitude of the transmitted wave takes the form

$$1 + f_+ = 1 + A + Be^{-ika} = \frac{2M(M+\beta)}{2M^2 + 2M\beta + \beta^2}. \tag{18}$$

It follows therefore that in the case of a purely nondiagonal disorder the amplitude $1 + f_+$ remains a real quantity and consequently the phase $\varphi = 0$. We note that in this case the amplitude f_- is real:

$$f_- = -(\beta^2 + 2M\beta)/(\beta^2 + 2M\beta + 2M^2). \tag{18a}$$

This caused by the asymmetrical character of the nondiagonal disorder. It changes nothing in the results, for in this case the initial equation (4) with V_{ms} from (3) is again transformed into Eq. (10) with $\varphi = 0$ by the substitution $R_m = (-1)^m r_m$, which leaves unchanged Eq. (5) for the state density. We note that this substitution leads to Eq. (10) with $\varphi = 0$ also in the case when $\varphi = \pi/2$. Therefore the condition for the appearance of the Dyson singularity is $\varphi = 0, \pi/2, \pi$.

A zero forward-scattering phase is possessed also by potentials of the form

$$u(x) = U(x) \cos 2p_0 x, \tag{19}$$

where $U(x)$ is a smooth function with a characteristic radius $b \gg p_0^{-1}$. It is shown in the Appendix that in this case

$$1 + f_+ = \frac{1}{\operatorname{ch} \alpha}, \quad f_- = i \operatorname{th} \alpha, \quad \alpha = \frac{1}{2v(\varepsilon)} \int_{-\infty}^{\infty} U(x)\, dx. \tag{20}$$

We shall not use hereafter the explicit expressions for γ and solve Eqs. (10) at $\varphi = 0$ and arbitrary $0 \leq \gamma \leq 1$.

4. SINGULARITY AT THE MIDDLE OF THE BAND

To determine the character of the singularity in the middle of the band, it is necessary to investigate in greater detail Eq. (10) at $\varphi = 0$. In the case of a weak potential, when $\gamma \ll 1$, Eq. (10) goes over into (see Ref. 6)

$$-itmR_m = 2m^2(R_{m+1} + R_{m-1} - 2R_m) + m(R_{m+1} - R_{m-1}). \tag{21}$$

It is easily seen that near the middle of the band, i.e., at $t \ll 1$, the major contribution is made in (21) by large $m \sim 1/t \gg 1$. In this limit we can therefore change from the discrete variable to the continuous $p = -itm$, and in the sums of (5) we can change from summation to integration. As a result, Eq. (21) takes the form

$$pR = 2p^2 \frac{d^2R}{dp^2} + 2p \frac{dR}{dp}. \tag{22}$$

This equation must be solved with the boundary conditions $R(0) = 1$ and $R(\infty) = 0$. It is easily seen that the solutions of (22) that decrease at infinity are of the form

$$R(p) = C_1 K_0((2p)^{1/2}). \tag{23}$$

At small $p \ll 1$ we have

$$K_0((2p)^{1/2}) \approx -{}^1/_2 \ln p.$$

Therefore in the principal logarithmic approximation, with account taken of the boundary condition $R(0) = 1$, which must now be imposed at $p \sim (-it)$, we have

$$C_1 = -2/\ln(-it). \tag{24}$$

Substituting (23) in (5) and replacing the summation by integration we obtain in the principal logarithmic approximation

$$\rho(t) \approx \rho_0 \frac{-4\pi}{|t| \ln^2 |t|}. \tag{25}$$

The character of the singularity of (25) coincides with Dyson's result for the phonon state density in a one-dimensional disordered chain.[3]

To determine the character of the singularity of $\rho(t)$ at arbitrary γ it is necessary to investigate in greater detail the solution of Eq. (10) in the region of large $m \sim 1/t \gg 1$. This can be done by the method developed

in a preceding paper.[7] It will be shown below that the sums over s in (10) converge rapidly and only values $s \sim 1$ are significant in them. At large m we can represent R_{m+s} in the form

$$R_{m+s}=\sum_{v=0}^{\infty}\frac{1}{v!}s^v\left(\frac{d}{dm}\right)^v R_m. \tag{26}$$

Writing for $(1-\gamma)^{2m-k}$

$$(1-\gamma)^{2m-k}=\sum_d C_{2m-k}^d(-\gamma)^d, \tag{27}$$

introducing the variable $n=k+s+d$, and representing s^v in the form

$$\left(a\frac{d}{da}\right)^v a^t|_{a=1},$$

we obtain for R_m the equation

$$-itmR_m=\frac{1}{\gamma}\sum_{v=0}^{\infty}\frac{1}{v!}V_v(m)\left(\frac{d}{dm}\right)^v R_m-\frac{1}{\gamma}R_m+\gamma^{m-1}, \tag{28}$$

$$V_v(m)=\sum_{k,n,d}C_{2m}^k C_{2m+2n-2k-2d-1}^{2n-k-2d}C_{2m-k}^d(-1)^{k+d}\gamma^n\left(a\frac{d}{da}\right)^v a^{n-k-d}|_{a=1}. \tag{29}$$

Representing $C_{2m+2n-2k-2d-1}^{2n-k-2d}$ in the form

$$C_{2m+2n-2k-2d-1}^{2n-k-2d}=\frac{1}{2\pi i}\oint\frac{dz}{z^{1+2n-k-2d}(1-z)^{2m-k}}, \tag{30}$$

where the integration is over a circle of radius $\rho<1$ around zero, we get

$$-itmR_m=\sum_{n,v=1}^{\infty}\frac{\gamma^{n-1}}{v!}\left(a\frac{d}{da}\right)^v|_{a=1}\frac{1}{2\pi i}\oint\frac{dz}{z^{2n+1}}\left(\frac{a-z}{a(1-z)}\right)^{2m}$$

$$\times a^{-n}\left(\frac{d}{dm}\right)^v R_m. \tag{31}$$

At large m

$$\left(a\frac{d}{da}\right)^v|_{a=1}\frac{1}{2\pi i}\oint\frac{dz}{z^{2n+1}}\left(\frac{a-z}{a(1-z)}\right)^{2m}a^{-n}\approx$$

$$\approx\frac{(2m)^v}{2\pi i}\oint\frac{dz}{z^{2n+1}}\left(\frac{z}{1-z}\right)^v. \tag{32}$$

It follows therefore that the equation for R_m at large m contains as before only terms of the type $m^v(d/dm)^vR_m$. Therefore, making the substitution $p=-itm$ and first summing over n and then integrating with respect to z, we obtain for $R(p)$ the equation

$$pR=\frac{1}{2\gamma}\sum_{v=1}^{\infty}\frac{1}{v!}\left[\left(\frac{\gamma^{1/2}}{1-\gamma^{1/2}}\right)^v+\left(\frac{-\gamma^{1/2}}{1+\gamma^{1/2}}\right)^v\right](2p)^v\left(\frac{d}{p}\right)^v R. \tag{33}$$

It is easily seen that $R(p)\approx A\ln p$ at small $p\ll 1$. Therefore, taking into account the boundary condition $R(0)=1$, which must now be imposed at $p\sim(-it)$, we have $A=1/\ln(-it)$. From this, in particular, it follows that near the middle of the band the state density $\rho(t)$ has a singularity of the Dyson type

$$\rho(t)\approx\rho_0\frac{-2\pi}{|t|\ln^2|t|}B(\gamma), \tag{34}$$

where

$$B(\gamma)=\int_0^{\infty}R_B^2(p)\,dp, \tag{35}$$

and $R_B(p)$ is the solution of (33) with the boundary condition $R_B(p)=\ln p$ as $p\to 0$.

In the general case the solution of (33) can be represented as series in powers of p:

$$R_B(p)=\sum_{n=0}^{\infty}(a_n\ln p+b_n)p^n,\quad a_0=1. \tag{36}$$

The coefficients a_n and b_n are represented by the recursion relations

$$2(z-1)^2a_{n-1}=(z+1)^2(z^n+z^{-n}-2)a_n, \tag{37}$$

$$2(z-1)^2b_{n-1}=(z+1)^2[(z^n+z^{-n}-2)b_n+\ln z(z^n-z^{-n})a_n], \tag{38}$$

$$z=(1+\gamma^{1/2})/(1-\gamma^{1/2}).$$

The quantities a_n are determined completely by the boundary condition $a_0=1$. The quantity b_0 is determined by the condition that $R(p)$ decrease at infinity (in particular, at $\gamma\ll 1$ the coefficient $b_0=2C-\ln 2$, where $C=0.577\ldots$ is the Euler constant).

It is easily seen that the function $R(p)$ defined by expansion (36) and by the recursion relations (37) and (38) satisfies the functional equation

$$2(z-1)^2pR(p)=(z+1)^2[R(pz)+R(p/z)-2R(p)]. \tag{39}$$

It follows from (39), in particular, that $R(p)$ decreases quite rapidly at large p. In fact, substituting in (39) $R(p)=e^{-\zeta(p)}$ we get at $p\gg 1$, in the principal logarithmic approximation,

$$\zeta(p)\approx\ln^2 p/2\ln z. \tag{40}$$

Equation (39) can be easily solved by the method developed in Ref. 10. A plot of $B(\gamma)$ is shown in Fig. 3. It is seen from this plot that when γ increases from 0 to 1 the coefficient $B(\gamma)$ increases quite rapidly and becomes infinite as $\gamma\to 1$.

By using numerical methods it is also easy to solve Eqs. (10). To this end it is necessary to use the rapid convergence of the sums over m and terminate the system of equation at a large $M\gg 1$, setting all the R_m with $m>M$ equal to zero. The resultant system of linear equation is easy to solve numerically. Plots of $\rho(t)$ at $\varphi=0$ and γ equal to 0.01, 0.7, and 0.99 are shown in Fig. 4. We note that with increasing γ the enhancement of the singularity at the center of the band is preceded by a minimum of the state density. The reason is that the total number of states in the chain remains unchanged and

$$\int_{-\infty}^{\infty}dt(\rho(t)-\rho_0)=0. \tag{41}$$

With the aid of this condition we easily find the asymptotic form of $B(\gamma)$ as $\gamma\to 1$.

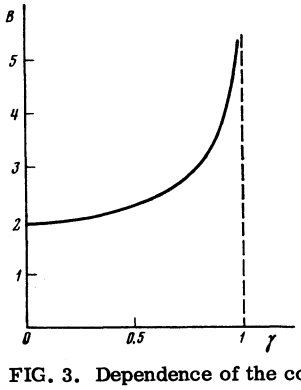

FIG. 3. Dependence of the coefficient of the Dyson singularity on γ.

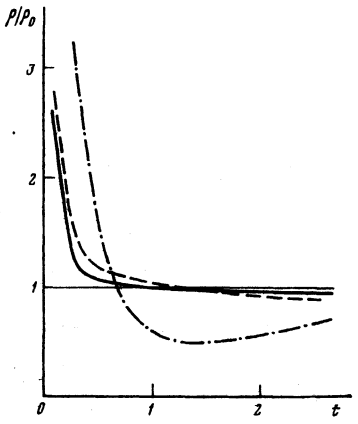

FIG. 4. Distribution of state density at the center of the band at $\varphi = 0$ and $\gamma = 0.01$ (solid line), $\gamma = 0.7$ (dashed), and $\gamma = 0,99$ (dash-dot line).

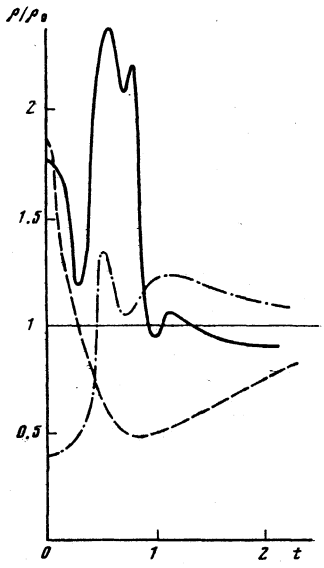

FIG. 5. Distribution of the state density at the center of the band in the case of a δ-function potential ($\sin\varphi = \gamma^{1/2}$) at $\gamma = 0.5$ (dashed line), $\gamma = 0.9$ (dash-dot line), and $\gamma = 0.99$ (solid).

In fact, in the region $t \neq 0$ it is easy to solve Eq. (10) as $\gamma \to 1$. Retaining in it only the terms of lowest order in $1-\gamma \ll 1$, we get

$$R_m = (1-itm)^{-1}. \tag{42}$$

Substituting (42) in (5) we get at $t \neq 0$

$$\rho(t) = \rho_0 \left[\frac{\pi}{t\,\mathrm{sh}(\pi/t)}\right]^2. \tag{43}$$

This solution is valid only at $t \neq 0$. In fact, for any finite $1-\gamma$ the solution (42) is not valid in the region $|t| \lesssim (1-\gamma)^{1/2}$. There is consequently a δ-function peak at the center of the band. The coefficient 2π of the δ function is determined from the condition (41). Therefore at $\gamma = 1$

$$\rho(t) = \rho_0 \left[2\pi\delta(t) + \left(\frac{\pi}{t\,\mathrm{sh}(\pi/t)}\right)^2\right]. \tag{44}$$

The onset of the δ-function peak as $\gamma \to 1$ is quite obvious, for if the electron is solidly locked-in its spectrum becomes strictly discrete, and only states with momentum $p = \pi/2a$ are left near the center of the band. Since the integral of the singular term equals 2π as $\gamma \to 1$, its estimated value at logarithmic accuracy is

$$(-2\pi B(\gamma)) \int_{-t_0}^{t_0} \frac{dt}{|t|\ln^2|t|} = \frac{2\pi B(\gamma)}{\ln^2 t_0}, \quad t_0 \sim (1-\gamma)^{1/2}. \tag{45}$$

Therefore as $\gamma \to 1$

$$B(\gamma) \approx {}^1/_4 \ln^2(1-\gamma). \tag{46}$$

We note that as $\gamma \to 1$ the expression (44) for the state density is universal and does not depend on the phase φ. This is easily seen from Eq. (4) by recognizing that as $\gamma \to 1$ we have $f_- \to (-1)$. The last circumstance is brought about by the fact that for infinitely strong scatterers the wave function is $\psi(x) = A\sin px$ and therefore $f_- = -1$. Since the function $\rho(t)$ has a δ-function singularity at the center of the band at $\gamma = 1$, the center of the band has at finite values of the parameter $1-\gamma$ and at arbitrary phases a state-density peak whose height tends to infinity as $\gamma \to 1$. By way of example, Fig. 5 shows the structure of the peak for a δ-function potential $u(x)$ ($\sin\varphi = \gamma^{1/2}$) at $\gamma = 0.5$, 0.9, and 0.99. We note that the structure of $\rho(t)$ is in this quite complicated and has several local maxima and minima. It must be emphasized that the state density reaches relatively slowly its limiting distribution (44) as $\gamma \to 1$. At certain values of γ, as seen from Fig. 5, there is a noticeable dip of the state density near the middle of the band.

5. STATE-DENSITY PEAKS AT RATIONAL POINTS OF THE BAND

In the limit of infinitely strong scatterers, δ function peaks of the state density occur at all rational points of the band. This is due to the strictly discrete character of the spectrum in wells with infinite walls, which cause the state density to differ from zero only at the rational points of the band. Inasmuch as at $\gamma \to 1$ the height of the peaks at the rational points becomes infinite, one can expect this height to be quite large at a finite but small value of $1-\gamma$.

The equations for the quantities R_m, which determine in accord with (5) the state-density change due to the disorder, are obtained in complete analogy with expression (2). It must only be recognized here that at $p_0 = \pi M/an$ ($1 \leq M \leq n-1$, $n = 2, 3, 4\ldots$) the change of the number of line pairs in the cross section must be a multiple of n. As a result we obtain readily

$$-\frac{d}{dx}R_m = c\sum_s V_{ms}R_{m+s}e^{2is(p_0-p)x} - cR_m + cR_0 f_-^{nm} e^{2inm(p-p_0)x}, \tag{47}$$

$$V_{ms} = \sum_k C_{nm}^{k} C_{nm+ns-1}^{k+ns}(f_-)^{2k+ns}(1+f_+)^{2nm-2k}. \tag{48}$$

The substitution $R_m(x) = R_m e^{2inm(p-p_0)x}$ and the use of relations (6)–(9) for f_+ and f_- reduces (47) to the form

$$-itmR_m = \frac{1}{\gamma}\sum_s V_{ms}R_{m+s} - \frac{1}{\gamma}R_m + \gamma^{nm/2-1}e^{inm(\varphi+\pi/2)}, \tag{49}$$

$$V_{ms}=\sum_k C_{nm}^{\,k} C_{nm+ns-1}^{\,k+ns}(-1)^k\gamma^{ns/2+k}$$
$$\times(1-\gamma)^{nm-k}e^{in(\varphi(2m+s)+sn/2)}, \tag{50}$$

$$t=2n(p-p_0)l\,. \tag{51}$$

In the limit as $\gamma\to 1$ Eqs. (49) can be solved exactly and lead to Eq. (44). This is easily seen from (47) by recognizing that as $\gamma\to 1$ we have $f_-\to(-1)$. In the limit of small $\gamma\to 1$ Eqs. (49) result in only small corrections on the order of $\gamma^{n/2-1}$ to the state density ρ_0. At $\gamma\sim 1$ it is easy to solve Eqs. (49) numerically. The plots of $\rho(t)$ obtained in this manner for $n=4$, $\varphi=0$, and $\gamma=0.5$, 0.7, and 0.9 are shown in Fig. 6. We note that although the state-density peaks have a finite height in this case, they are strong enough to lead to significant effects.

6. CONCLUSION

We note in conclusion that the state density $\rho(\varepsilon_F)$ at the Fermi level and its dependence on ε near ε_F influence substantially the magnitude and the temperature dependence of the magnetic susceptibility χ, which is described by the formula

$$\chi(T)=2\mu_B^2\int_{-\infty}^{\infty}\frac{d\varepsilon}{4T}\operatorname{ch}^{-2}\left(\frac{\varepsilon}{2T}\right)\rho(\varepsilon), \tag{52}$$

where μ_B is the Bohr magneton.

The state-density peaks on the Fermi level increase the susceptibility at low temperatures. In TCNQ salts with strong structural disorder such an increase was in fact observed.[9] The degree of filling of the electron band in these salts is either 1/2(NMP-TCNQ) or 1/4[Qn(TCNQ)$_2$, Ad(TCNQ)$_2$]. Recent estimates of the random potential u in these substances[11] show that $u\approx 0.34$ eV in Qn(TCNQ)$_2$ and $u\approx 0.17$ eV in Ad(TCNQ)$_2$. The half-width M of the band in these substances is approximately 0.15 eV.[12] Therefore the parameter α that determines the strength of the interaction between the electron and the impurity according to the formula $\alpha=ua/v_F$ is ~1.5 in Ad(TCNQ)$_2$ and ~3 in Qn(TCNQ)$_2$. This points to a strong character of the electron scattering in the TCNQ salts with asymmetrical cations, and is in good agreement with estimates of the mean free path of the electron in these substances, made on the basis of the dielectric constant.[7] The strong scattering of the electrons should result in a strong peak of the state density with height $\sim 10\rho_0$ and width ~5 K near 1/4 of the band and explains in principle the growth of $\chi(T)$. It is difficult at present, in view of the insufficient data on the random potential, to compare in detail the theoretical and experimental $\chi(T)$ dependences, since the lack of data does not make it possible to determine the connection between α and the reflection coefficient γ, whose value influences very strongly the $\rho(\varepsilon)$ dependence.

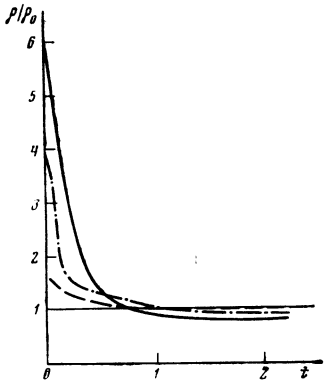

FIG. 6. State-density distribution near $\frac{1}{4}$ of the band at $\varphi=0$ and $\gamma=0.5$ (dashed line), $\gamma=0.7$ (dash-dot line), and $\gamma=0.9$ (solid).

The distribution of the electronic state density was investigated by a computer simulation method.[13-17] This revealed[16,17] a singularity of the state density near the band center in systems with purely nondiagonal disorder. Investigations were made[13-15] of systems with diagonal disorder, and the presence of state-density peaks near 1/6 and 1/4 of the band was observed.

In conclusion, the author thanks L. P. Gor'kov, O. N. Dorokhov, V. I. Mel'nikov, and É. I. Rashba for a useful discussion of the results.

APPENDIX

To find expressions for the amplitudes f_+ and f_- we use a diagram expansion in terms of the impurity potential. In the coordinate representation, one of the first diagrams for f_+ and f_- is shown in Fig. 7. The characteristic scale of integration with respect to x_i is $(x_i-x_j)\sim b\gg p_0^{-1}$. Therefore integration of $\cos 2p_0x$ over a scale larger than p_0^{-1} but smaller than b causes vanishing of the Born zero-angle scattering amplitudes. The integrals of $u(x)\sin 2p_0x$ vanish similarly. As a result we obtain for the amplitudes f_+ and f_-, with allowance for the conditions $x_{2k}<x_{2k+1}$, $x_{2k+2}<x_{2k+1}$ the expressions

$$f_+=\sum_{k=1}^{\infty}\Phi_{2k},\quad f_-=\sum_{k=1}^{\infty}\Phi_{2k-1}; \tag{A.1}$$

$$\Phi_{2k}=\int_{-\infty}^{\infty}dx_{2k}u_1(x_{2k})\int_{x_{2k}}^{\infty}dx_{2k-1}u_1(x_{2k-1})\int_{-\infty}^{x_{2k-1}}dx_{2k-2}u_1(x_{2k-2})\ldots\int_{x_2}^{\infty}dx_1u_1(x_1), \tag{A.2}$$

$$\Phi_{2k-1}=\int_{-\infty}^{\infty}dx_{2k-1}u_1(x_{2k-1})\int_{-\infty}^{x_{2k-1}}dx_{2k-2}u_1(x_{2k-2})$$
$$\times\int_{x_{2k-2}}^{\infty}dx_{2k-3}u_1(x_{2k-3})\ldots\int_{x_2}^{\infty}dx_1u_1(x_1),$$

where

$$u_1(x)=\frac{i}{v(\varepsilon)}u(x)\cos 2p(\varepsilon)x.$$

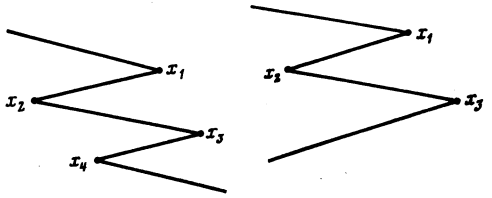

FIG. 7.

Introducing the function

$$\Phi(x)=\int_{-\infty}^{x} u_1(y)\,dy$$

and integrating (A.2) the required number of times by parts, with allowance for the boundary conditions $\Phi(-\infty)=0$, $\Phi(+\infty)=ia$ we get the following recursion relations for Φ_n:

$$\Phi_{2k}=\sum_{n=1}^{k}\Phi_{2k-2n}(-1)^{n+1}\frac{(i\alpha)^{2n}}{(2n)!}, \tag{A.3}$$

$$\Phi_{2k-1}=\sum_{n=1}^{k}\Phi_{2k-2n}(-1)^{n+1}\frac{(i\alpha)^{2n-1}}{(2n-1)!}. \tag{A.4}$$

These equations must be solved with the boundary condition $\Phi_0=1$. Summing (A.3) and (A.4) over k, we obtain for f_+ the equation

$$f_+=(1+f_+)\sum_{n=1}^{\infty}(-1)^{n+1}\frac{(i\alpha)^{2n}}{(2n)!}, \tag{A.5}$$

from which it follows that

$$1+f_+=\frac{1}{\operatorname{ch}\alpha},\quad f_-=i\operatorname{th}\alpha,\quad \alpha=\frac{1}{2v}\int_{-\infty}^{\infty}U(x)\,dx. \tag{A.6}$$

[1]I. F. Shchegolev, Phys. Status Solidi A **12**, 9 (1972).
[2]S. A. Gredeskul and L. A. Pastur, Fiz. Nizk. Temp. **1**, 277 (1975) [Sov. J. Low Temp. Phys. **1**, 135 (1975)].
[3]F. Dyson, Phys. Rev. **92**, 1331 (1953).
[4]M. Weissman and N. V. Cohan, J. Phys. C: Solid State Phys. **8**, 145 (1975). T. P. Eggarter and R. Riedinger, Phys. Rev. **B18**, 569 (1978).
[5]A. A. Ovchinnikov and N. S. Érikhman, Pis'ma Zh. Eksp. Teor. Fiz. **25**, 197 (1977) [JETP Lett. **25**, 180 (1977)]; Zh. Eksp. Teor. Fiz. **73**, 650 (1977) [Sov. Phys. JETP **46**, 340 (1977)]. L. P. Gor'kov and O. N. Dorokhov, Fiz. Nizk. Temp. **4**, 332 (1978) [Sov. J. Low Temp. Phys. **4**, 160 (1978)]. S. A. Gredeskul and L. A. Pastur, Zh. Eksp. Teor. Fiz. **75**, 1444 (1978) [Sov. Phys. JETP **48**, 729 (1978)].
[6]A. A. Gogolin and V. I. Mel'nikov, Zh. Eksp. Teor. Fiz. **73**, 706 (1977) [Sov. Phys. JETP **46**, 369 (1977)].
[7]A. A. Gogolin, Zh. Eksp. Teor. Fiz. **76**, 1759 (1979) [Sov. Phys. JETP **49**, 895 (1979)].
[8]L. P. Gor'kov and O. N. Dorokhov, Solid State Commun. **20**, 789 (1976); **21**, 7 (1977).
[9]L. N. Bulaevskiĭ, A. V. Zvarykina, Yu. S. Karimov, P. B. Lyubovskiĭ, and I. F. Shchegolev, Zh. Eksp. Teor. Fiz. **62**, 725 (1972) [Sov. Phys. JETP **35**, 384 (1972)].
[10]A. A. Gogolin and V. I. Mel'nikov, Phys. Status Solidi B **88**, 377 (1978).
[11]K. Holczer, G. Mihaly, A. Janossy, G. Gruner, and M. Kertesz, J. Phys. C: Solid State Phys. **11**, 4707 (1978).
[12]A. A. Gogolin, S. P. Zolotukhin, V. I. Mel'nikov, É. I. Rashba, and I. F. Shchegolev, Pis'ma Zh. Eksp. Teor. Fiz. **22**, 564 (1975) [JETP Lett. **22**, 278 (1975)].
[13]R. L. Bush, Phys. Rev. **B6**, 1182 (1972).
[14]C. T. Papatriantafillou, Phys. Rev. **B7**, 5386 (1973).
[15]R. L. Agacy and R. E. Borland, Proc. Phys. Soc. London **84**, 320 (1964).
[16]J. E. Hirsch and T. P. Eggarter, Phys. Rev. **B14**, 2433 (1976).
[17]G. Theodorou and M. H. Cohen, Phys. Rev. **B13**, 4597 (1976).

Translated by J. G. Adashko